scientific reports

Check for updates

OPEN

UBTD1 is a potential prognostic biomarker in colorectal cancer

Zihan Zhao[1,2,5], Changjiang Yang[3,5], Xuhua Geng[1,2], Congrui Yuan[1,2], Ruoshen Yang[4] & Guibin Yang[1,2]✉

Colorectal cancer (CRC) is a complex malignancy with poorly understood molecular mechanisms, necessitating the identification of genetic markers. Although Ubiquitin domain-containing protein 1 (UBTD1) has received significant attention in the study of human cancers, its specific role in CRC is yet to be fully clarified. This study sought to examine how UBTD1 expression was associated with various clinical and pathological characteristics of CRC, and to determine its prognostic significance and biological function, utilizing data from clinical samples and large-scale databases. Notably, UBTD1 expression was found to be upregulated in CRC, resulting in decreased survival rates and unfavorable clinical characteristics such as advanced T, N, and pathological stages. The findings of the multivariate Cox regression analysis illustrated that UBTD1 expression upregulation is a significant independent marker of unfavorable outcomes in CRC patients. An examination of the functional enrichment of UBTD1 and the genes it co-expresses indicated that it could serve as an oncogene by modulating the expression of genes implicated in crucial tumorigenesis pathways and functions. Additionally, immune cell infiltration analysis suggested a link between UBTD1 levels and various immune cells, particularly macrophages. In conclusion, the use of UBTD1 as a biomarker for both the prognosis and diagnosis of CRC has promising prospects for further investigation and therapeutic approaches.

Keywords Ubiquitin domain-containing protein 1, Colorectal cancer, Immune microenvironment, Prognosis

Colorectal cancer (CRC) is a gastrointestinal tract-associated malignancy that is widely prevalent and has emerged as one of the most frequently occurring tumors on a global scale. An estimated 19.3 million new cases of CRC are diagnosed annually on a global scale, resulting in approximately 10 million deaths[1,2]. Recent reviews[3,4] have pointed out that the CRC incidence rate exhibits regional variations globally, particularly in regions with a low socioeconomic index or undergoing developmental transition, resulting in significant economic and healthcare burdens. Timely detection and treatment of tumors are essential for enhancing CRC outcomes, underscoring the importance of identifying novel biomarkers for early detection and prognosis improvement[5–7]. Consequently, there is a significant emphasis on conducting additional research to elucidate the pathogenesis and underlying factors contributing to CRC. Ubiquitination is a critical post-translational modification with an essential function in protein degradation and functional regulation. The covalent attachment of ubiquitin to target proteins is critically involved in several cellular processes, such as signal transduction, protein sorting, gene expression, and mitosis[8]. Ubiquitin domain-containing protein 1 (UBTD1) is a highly conserved ubiquitin-like protein that interacts with specific E2 and E3 enzymes of the ubiquitin–proteasome system (UPS) in both in vitro and in vivo settings[9]. Research has demonstrated that upregulation of UBTD1 can trigger senescence in human fibroblasts and cancer cells, thereby reducing the oncogenic properties of the cancer cells[10]. Furthermore, UBTD1 has been shown to enhance the stability of the tumor suppressor p53 protein through the facilitation of Mdm2 protein degradation. The depletion of UBTD1 has been found to significantly influence the mechanical characteristics of epithelial cancer cells by activating RhoA, thereby fostering their aggressive behavior[11,12]. Moreover, UBTD1 is mainly implicated in the processes of epidermal growth factor receptor (EGFR) self-phosphorylation and subsequent lysosomal degradation. Depletion of UBTD1 leads to heightened EGFR signaling and increased cell proliferation. Additionally, UBTD1 plays a role in the proteasome-mediated degradation of YAP, a key cell mechano-transducer. UBTD1 downregulation contributes to a dismal prognosis and a highly aggressive phenotype, indicating its potential as a treatment target for inhibiting cancer progression[13].

[1]Department of Gastroenterology, Aerospace Center Hospital, 15 Yuquan Road, Haidian District, Beijing 100049, China. [2]Peking University Aerospace School of Clinical Medicine, Beijing, China. [3]Department of Gastroenterological Surgery, Peking University People's Hospital, Beijing, China. [4]School of Computer Science and Engineering, Beijing Technology and Business University, Beijing, China. [5]These authors contributed equally: Zihan Zhao and Changjiang Yang. ✉email: yanggb@sina.com

Nevertheless, the function of UBTD1 in CRC is still largely undefined and lacks comprehensive characterization. To address this question, we evaluated the UBTD1 expression in CRC and normal tissues by utilizing the Gene Expression Omnibus (GEO) and The Cancer Genome Atlas (TCGA) databases. Moreover, our study sought to determine the clinical value of UBTD1 in CRC patients through an analysis of its relationship with individual patient characteristics and survival rates. Furthermore, we probed into the connection between UBTD1 mRNA expression levels and the tumor immune microenvironment (TIME) to enhance our understanding of UBTD1's role in anti-tumor immunity and the progression of CRC.

Materials and methods

Collection and preprocessing of data

TCGA (https://cancergenome.nih.gov/) (accessed on 1 December 2023)) was queried to compile RNA-Seq data on gene expression and pertinent clinical information from normal and malignant tissues in rectum adenocarcinoma (READ) and colon adenocarcinoma (COAD). In this investigation, GSE22598 and GSE110224 were selected and extracted from GEO (http://www.ncbi.nlm.nih.gov/geo (accessed on 1 December 20222023)).

Survival analysis

The Kaplan–Meier (KM) technique and log-rank test were employed for survival analyses, with the threshold set as the median UBTD1 expression level. The assessment of how the patient outcomes correlated with clinical and pathological variables was conducted via univariate and multivariate Cox regression analyses. We considered prognostic variables in the ensuing multivariate analysis if their p-value was < 0.1 in the univariate analysis. The next step was to find independent prognostic markers via multivariate Cox analysis.

Enrichment analysis

The study examined the biological function of UBTD1 in CRC by conducting differential gene expression analyses (DEGs) on low- and high-expression groups, with $|\log FC| > 1$ and FDR < 0.05 as thresholds for significance. Functional enrichment analysis of Gene Ontology (GO) and Kyoto Encyclopedia of Genes and Genomes (KEGG), as well as gene set enrichment analysis (GSEA), was executed utilizing the ClusterProfiler tool in R (version 3.6.3). The GO analysis encompassed molecular functions (MFs), cellular components (CCs), and biological processes (BPs). Notably, GSEA is a computational platform for evaluating the statistical significance and agreement of differences between two biological conditions predicated on a predefined gene set. For each phenotype, the enriched pathways were classified utilizing a normalized enrichment score (NES) and an adjusted p-value. The c2.cp.kegg.v2022.1.Hs.symbols.gmt [KEGG Pathway Database] was the reference gene set for the KEGG pathways. Additionally, c5.go.all.v2022.1.Hs.symbols.gmt [GO] (10561) was selected to be the GO term reference gene set. The gene sets were deemed to undergo significant enrichment when the adjusted p-value was < 0.05 and the false discovery rate (FDR) was < 0.25.

Immune infiltration analyses

The ESTIMATE algorithm was utilized to determine the immune and stromal scores of CRC[14]. Additionally, the CIBERSORT[15], EPIC[16], and QUANTISEQ[17] methods were employed to assess UBTD1's correlation with infiltrating immune cells. An evaluation of the link between UBTD1 expression and these immune cells was carried out via Spearman's correlation analysis. To assess the levels of immune cell infiltration in the low and high UBTD1 expression groups, we implemented the Wilcoxon rank-sum test.

Patients and clinical samples

Shanghai Outdo Biotech Company (Shanghai, China) provided the CRC tissue microarray (HColA160CS01) comprising 80 paired tumors and normal tissues. The Shanghai Outdo Biotech Company's Ethics Committee approved study protocols (ID: YB M-05-02).

Immunohistochemistry (IHC) staining

After fixing CRC and adjoining normal tissue sections in paraffin, they were subjected to dewaxing in dimethylbenzene followed by rehydration in ethanol at varying concentrations. Antigen was retrieved utilizing sodium citrate solution through microwave heating at 95 °C. Subsequently, the activity of endogenous peroxidase was effectively suppressed by adding 3% H_2O_2 to the sections for 10 min. Next, the tissue slices were incubated in a blocking solution and then exposed to 10% fetal bovine serum for one hour. Following incubation with the primary antibody UBTD1 (1:400; bs-7705R) all night at 4 °C, an HRP-labeled universal anti-rabbit secondary antibody was added to the sections to incubate them within a dark chamber. Subsequently, following the detection of immunostaining with diaminobenzidine (DAB), the sections underwent hematoxylin counterstaining, dehydration, and mounting. Thereafter, the assessment of UBTD1 expression levels was based on the percentage of positively stained cells and the intensity of the staining. Notably, the classification of positive cells included: 0 (0–10%), 1 (10–40%), 2 (40–70%), and 3 (> 70%), and staining intensity was coded as 1 (weak), 2 (moderate), and 3 (strong). Subsequently, the IHC scores for UBTD1 expression patterns were found by combining the proportion of cells that stained positively and how intensely they were stained. The definitive categorization of UBTD1 expression includes low (0–3) and high (4–6 points) expression. All procedures were conducted in compliance with applicable guidelines and regulations.

Statistical analysis

R 4.2.1 was utilized for analyzing the statistical data obtained from TCGA. To determine how UBTD1 levels varied in tumor and normal samples, we performed using both the Wilcoxon rank-sum and signed-rank tests. Additionally, Welch's one-way ANOVA with Bonferroni's post hoc test (or the t-test) was employed to determine the potential correlation of UBTD1 expression with clinical-pathological factors. The study utilized Pearson's chi-square test to investigate the impact of different clinicopathological variables on UBTD1 expression. Fisher's exact probability method was applied when the chi-square test categories did not satisfy the requirements of a total sample size > 40 or a theoretical frequency > 5. Additionally, a KM curve was generated to assess UBTD1's predictive capacity. Furthermore, Overall Survival (OS), Disease Specific Survival (DSS), and Progression Free Interval (PFI) were assessed using univariate and multivariate Cox regression models to determine the prognostic relevance of UBTD1 expression in conjunction with other clinicopathological factors. Variables showing significance in the univariate analysis were subsequently examined in the multivariate analysis. Receiver operating characteristic (ROC) analysis of UBTD1 was undertaken utilizing the pROC program. The recorded area under the curve (AUC) values within the range of 0.5–1.0 point to a discriminatory capacity ranging from 50 to 100%. Significance was observed for all tests with a two-tailed p-value of ≤ 0.05.

Ethics approval and consent to participate

This study was conducted with the approval of the Ethics Committee of Shanghai Outdo Biotech Company (ID: YB M-05-02).

Result

CRC is characterized by upregulated UBTD1 mRNA and protein levelsc

The study analyzed UBTD1 gene expression patterns in distinct human cancers and normal tissues utilizing TCGA-based data. The UBTD1 mRNA expression levels varied significantly between malignant cancers and their corresponding normal tissues, with notable distinctions observed in stomach adenocarcinoma (STAD), Thyroid carcinoma (THCA), Kidney Chromophobe (KICH), Prostate adenocarcinoma (PRAD), Liver hepatocellular carcinoma (LIHC), Lung squamous cell carcinoma (LUSC), Lung adenocarcinoma (LUAD), Kidney renal clear cell carcinoma (KIRC), and colon adenocarcinoma (COAD) (Fig. 1A,B). Specifically, UBTD1 was shown to be upregulated in CRC (Fig. 1C,D). Validation of UBTD1 expression was conducted utilizing supplementary GEO datasets (GSE22598, GSE110224). Analysis across these three disparate datasets revealed an upregulation of UBTD1 in CRC tissues in comparison with adjoining normal tissues (Fig. 1F,G). The AUC of the ROC curve for UBTD1 expression was established as 0.863 (95% CI 0.818–0.908), highlighting a promising predictive capacity for discriminating between tumor and normal samples (Fig. 1E). Subsequently, an IHC assay was utilized to evaluate UBTD1 expression in tumor and adjoining normal tissue specimens derived from CRC samples at Shanghai Outdo Biotech Company. In comparison with normal tissues, UBTD1 IHC scores in tumors were increased significantly, according to the findings (Fig. 1H,I).

UBTD1 expression is correlated with the CRC pathological stage

We probed into the UBTD1 expression patterns in 644 CRC patients from the TCGA database and investigated their associations with various clinical and pathological characteristics. By using Welch one-way ANOVA accompanied by Bonferroni's post-hoc test, the levels of UBTD1 expression were found to be significantly related to the T stage, N stage, and pathologic stage. Nevertheless, UBTD1 expression did not exhibit any statistically significant correlations with M stage, age, or gender (Fig. 2A–I). The threshold for stratifying the samples into low- and high-expression subgroups was established utilizing the median UBTD1 expression value. Subsequently, an evaluation was conducted to examine the association of UBTD1 expression in cancerous samples with a range of clinicopathological factors, such as clinical stage, T stage, distant metastasis, N stage, gender, age at diagnosis, OS, DSS, and PFI events. Table 1 presents a summary of UBTD1 expression correlations with clinicopathological features in 644 CRC patients. The patients with higher UBTD1 levels had more advanced pathological N stage, OS, DSS, and PFI events ($p = 0.001$, $p = 0.014$, $p < 0.001$, and $p = 0.015$, respectively) as opposed to those with lower levels. There were significant variations in the UBTD1 levels between the N stage ($p = 0.011$) and the pathological stage ($p = 0.022$) in the logistics association analysis (Table 2). Additionally, OS, DSS, and PFI times were all reduced in CRC patients with UBTD1 expression upregulation, according to the KM curves (Fig. 2J–L).

UBTD1 expression upregulation is correlated with unfavorable patient prognosis in CRC

Our study examined the prognostic value of UBTD1 in predicting OS, PFI, and DSS in CRC. Lower levels of UBTD1 were associated with improved OS, DSS, and PFI outcomes, as evidenced by KM survival analysis (Fig. 2J–L). The potential of UBTD1 expression and other clinicopathological features as independent risk factors for CRC patients was investigated utilizing univariate and multivariate models. According to the univariate analysis, most clinical features were strongly correlated with a negative OS, including age > 65 years ($p < 0.001$), T3 and T4 stages ($p = 0.004$), N1 and N2 stages ($p < 0.001$), M1 stage ($p < 0.001$), TNM III/IV stages ($p < 0.001$), and UBTD1 expression upregulation ($p = 0.003$). The same results are reflected in multivariate analysis (Table 3). Additionally, T3 and T4 stages ($p = 0.002$), N1 and N2 stages ($p < 0.001$), M1 stage ($p < 0.001$), and UBTD1 expression upregulation ($p < 0.001$) were strongly correlated with reduced DSS in the univariate analysis. Furthermore, the M stage ($p < 0.001$), TNM III/IV stages ($p = 0.013$), and UBTD1 levels ($p = 0.023$) independently act as OS predictors in the multivariate analysis (Table 4). It was also found that T3 and T4 stages ($p < 0.001$), N1 and N2 stages ($p < 0.001$), M1 stage ($p < 0.001$), TNM III/IV stages ($p < 0.001$), and UBTD1 expression upregulation ($p = 0.002$) significantly correlated with a reduced PFI in the univariate analysis. Moreover, the independent

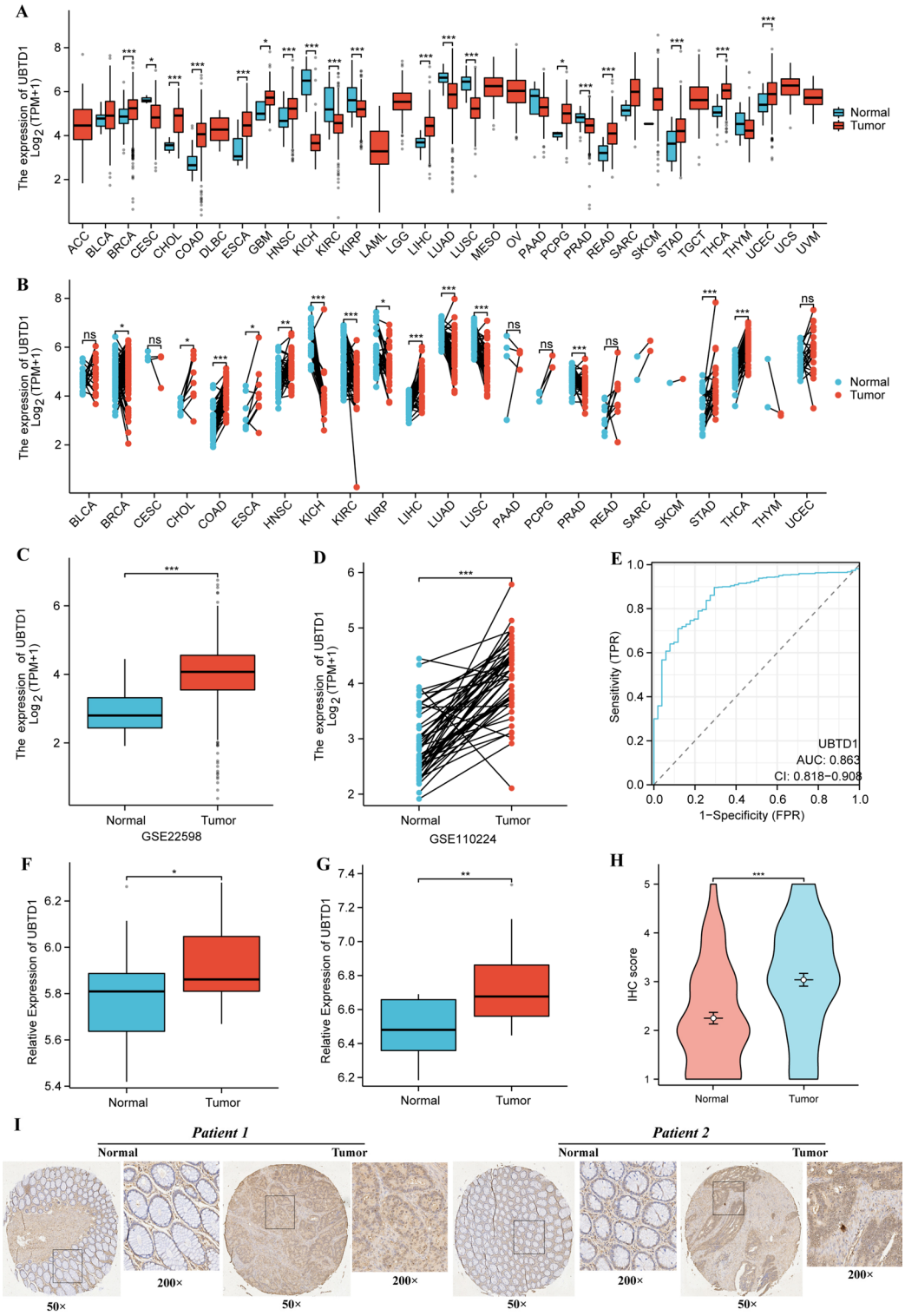

Figure 1. The levels of UBTD1 protein and mRNA expression in pan-cancer and CRC relative to normal samples. (**A**, **B**) Comparative analysis of UBTD1 mRNA expression in pan-cancer and normal tissues using TCGA. (**C**, **D**) TCGA analysis illustrated that UBTD1 mRNA expression was upregulated in CRC in comparison with normal samples. (**E**) The diagnostic value of UBTD1 ROC analysis in CRC. (**F**, **G**) GEO findings indicate an upregulation of UBTD1 mRNA expression in CRC in comparison with normal samples. (**H**, **I**) UBTD1 protein expression was upregulated in CRC in comparison with normal samples, as shown by immunohistochemistry. (ns denotes no significance, *p < 0.05, **p < 0.01, ***p < 0.001).

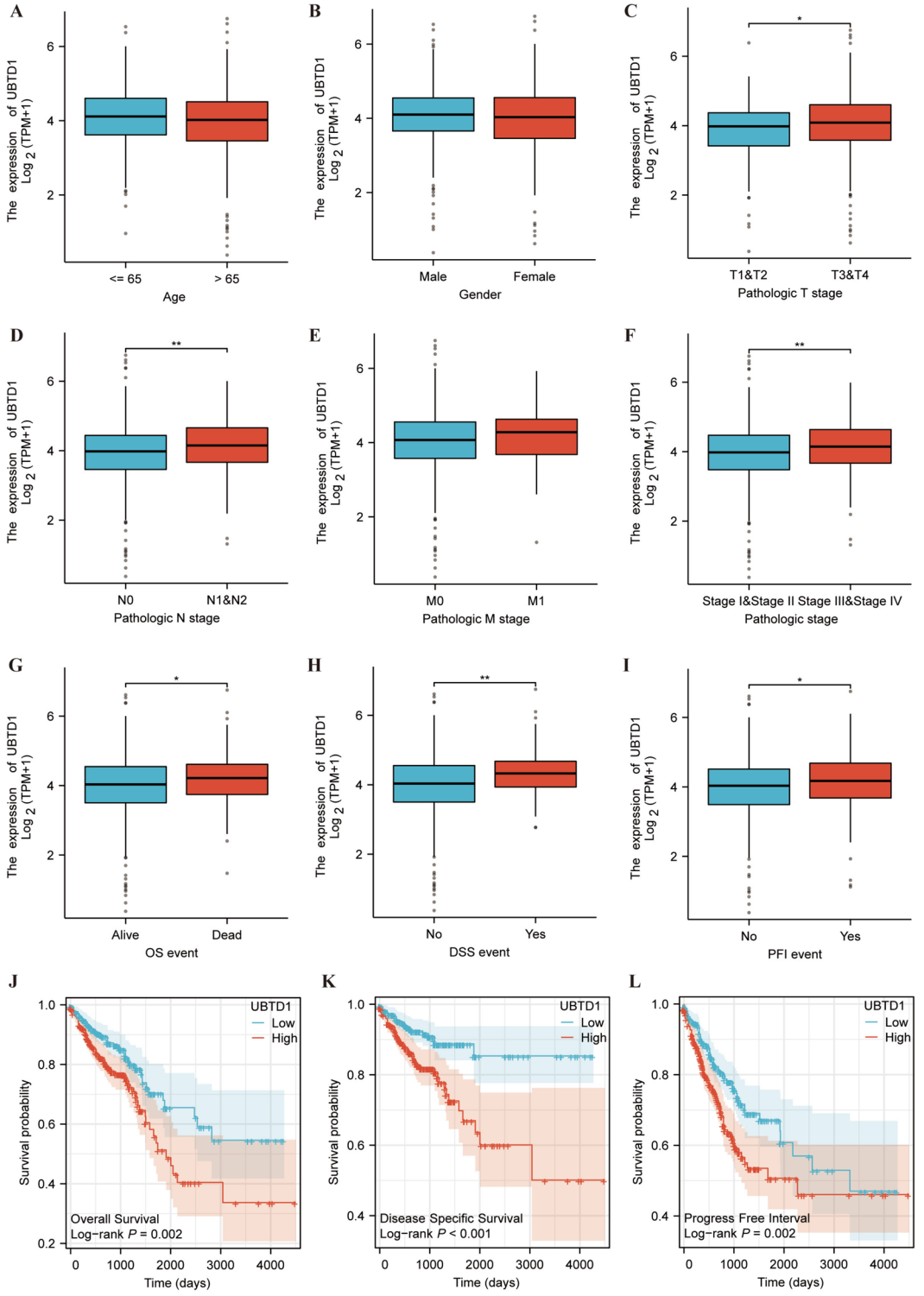

Figure 2. TCGA database-based correlations between UBTD1 expression and clinicopathologic parameters and prognosis in CRC. (**A**–**I**) Significant association of UBTD1 expression with T stage (**C**), N stage (**D**), and pathological stage (**F**) as well as OS (**G**), DSS (**H**), and PFI (**I**). (**J**–**L**) UBTD1 expression upregulation was related to reduced OS, DSS, and PFI times, as indicated by the Kaplan–Meier curves. (ns represents no significance, *p < 0.05, **p < 0.01, ***p < 0.001).

Characteristics	Low expression of UBTD1	High expression of UBTD1	p value
n	322	322	
Pathologic T stage, n (%)			0.470
T1	12 (1.9%)	8 (1.2%)	
T2	60 (9.4%)	51 (8%)	
T3	214 (33.4%)	222 (34.6%)	
T4	33 (5.1%)	41 (6.4%)	
Pathologic N stage, n (%)			0.001
N0	200 (31.2%)	168 (26.2%)	
N1	78 (12.2%)	75 (11.7%)	
N2	42 (6.6%)	77 (12%)	
Pathologic M stage, n (%)			0.130
M0	239 (42.4%)	236 (41.8%)	
M1	37 (6.6%)	52 (9.2%)	
Pathologic stage, n (%)			0.108
Stage I	61 (9.8%)	50 (8%)	
Stage II	128 (20.5%)	110 (17.7%)	
Stage III	86 (13.8%)	98 (15.7%)	
Stage IV	37 (5.9%)	53 (8.5%)	
Gender, n (%)			0.236
Female	158 (24.5%)	143 (22.2%)	
Male	164 (25.5%)	179 (27.8%)	
Age, n (%)			0.152
≤65	129 (20%)	147 (22.8%)	
>65	193 (30%)	175 (27.2%)	
OS event, n (%)			0.014
Alive	270 (41.9%)	245 (38%)	
Dead	52 (8.1%)	77 (12%)	
DSS event, n (%)			<0.001
No	281 (45.2%)	263 (42.3%)	
Yes	24 (3.9%)	54 (8.7%)	
PFI event, n (%)			0.015
No	253 (39.3%)	226 (35.1%)	
Yes	69 (10.7%)	96 (14.9%)	

Table 1. The association of UBTD1 expression with clinicopathological features in the TCGA cohort.

Characteristics	Total (N)	OR (95% CI)	p value
Pathologic T stage (T3 & T4 vs. T1 & T2)	641	1.299 (0.884–1.911)	0.183
Pathologic N stage (N1 & N2 vs. N0)	640	1.508 (1.100–2.067)	0.011
Pathologic M stage (M1 vs. M0)	564	1.423 (0.900–2.251)	0.131
Pathologic stage (Stage III & Stage IV vs. Stage I & Stage II)	623	1.450 (1.055–1.993)	0.022
Age (>65 vs. ≤65)	644	0.796 (0.582–1.088)	0.152
Gender (male vs. female)	644	1.206 (0.885–1.644)	0.236

Table 2. Logistics association between UBTD1 expression and clinicopathologic features.

function of the T3 and T4 stages ($p = 0.042$), M stage ($p < 0.001$), and UBTD1 expression upregulation ($p = 0.040$) in predicting PFI were shown in the multivariate analysis (Table 5).

Potential involvement of UBTD1 in CRC malignant progression

We initially selected the 50 top-ranked significantly correlated genes with UBTD1, as illustrated in the heatmap, to explore the biological activities of UBTD1 in CRC (Fig. 3A). Subsequently, these genes were subjected to GO and KEGG analyses. Additionally, the following were found to be predominantly linked to co-expressed genes that exhibited a correlation coefficient > 0.6 with UBTD1, as indicated by the GO term annotation: collagen-containing extracellular matrix (ECM), ECM organization, collagen metabolic process, extracellular structure

Characteristics	Total (N)	Univariate analysis		Multivariate analysis	
		Hazard ratio (95% CI)	p value	Hazard ratio (95% CI)	p value
Pathologic T stage	640				
T1 & T2	131	Reference		Reference	
T3 & T4	509	2.468 (1.327–4.589)	0.004	2.219 (1.009–4.880)	0.048
Pathologic N stage	639				
N0	367	Reference		Reference	
N1 & N2	272	2.627 (1.831–3.769)	< 0.001	0.360 (0.136–0.952)	0.039
Pathologic M stage	563				
M0	474	Reference		Reference	
M1	89	3.989 (2.684–5.929)	< 0.001	2.310 (1.430–3.731)	< 0.001
Pathologic stage	622				
Stage I & Stage II	348	Reference		Reference	
Stage III & Stage IV	274	2.988 (2.042–4.372)	< 0.001	5.793 (1.973–17.014)	0.001
Gender	643				
Female	301	Reference			
Male	342	1.054 (0.744–1.491)	0.769		
Age	643				
≤ 65	276	Reference		Reference	
> 65	367	1.939 (1.320–2.849)	< 0.001	3.022 (1.930–4.731)	< 0.001
UBTD1	643				
Low	321	Reference		Reference	
High	322	1.723 (1.210–2.452)	0.003	1.751 (1.178–2.602)	0.006

Table 3. The univariate and multivariate analyses of OS.

Characteristics	Total (N)	Univariate analysis		Multivariate analysis	
		Hazard ratio (95% CI)	p value	Hazard ratio (95% CI)	p value
Pathologic T stage	618				
T1 & T2	129	Reference		Reference	
T3 & T4	489	6.440 (2.029–20.441)	0.002	2.734 (0.830–9.009)	0.098
Pathologic N stage	617				
N0	358	Reference		Reference	
N1 & N2	259	4.119 (2.496–6.797)	< 0.001	0.511 (0.195–1.336)	0.171
Pathologic M stage	542				
M0	455	Reference		Reference	
M1	87	7.471 (4.647–12.012)	< 0.001	3.726 (2.075–6.693)	< 0.001
Pathologic stage	601				
Stage I & Stage II	339	Reference		Reference	
Stage III & Stage IV	262	5.716 (3.240–10.083)	< 0.001	4.502 (1.372–14.774)	0.013
Gender	621				
Female	290	Reference			
Male	331	1.207 (0.769–1.895)	0.412		
Age	621				
< = 65	273	Reference			
> 65	348	1.421 (0.894–2.257)	0.137		
UBTD1	621				
Low	304	Reference		Reference	
High	317	2.420 (1.496–3.917)	< 0.001	1.816 (1.084–3.041)	0.023

Table 4. The univariate and multivariate analyses of DSS.

Characteristics	Total (N)	Univariate analysis		Multivariate analysis	
		Hazard ratio (95% CI)	P value	Hazard ratio (95% CI)	P value
Pathologic T stage	640				
T1 & T2	131	Reference		Reference	
T3 & T4	509	3.198 (1.814–5.636)	< 0.001	1.855 (1.024–3.360)	0.042
Pathologic N stage	639				
N0	367	Reference		Reference	
N1 & N2	272	2.624 (1.916–3.592)	< 0.001	0.888 (0.378–2.086)	0.785
Pathologic M stage	563				
M0	474	Reference		Reference	
M1	89	5.577 (3.945–7.884)	< 0.001	4.411 (2.825–6.885)	< 0.001
Pathologic stage	622				
Stage I & Stage II	348	Reference		Reference	
Stage III & Stage IV	274	2.924 (2.115–4.044)	< 0.001	1.389 (0.537–3.593)	0.498
Gender	643				
Female	301	Reference			
Male	342	1.217 (0.892–1.660)	0.216		
Age	643				
≤ 65	276	Reference			
> 65	367	1.006 (0.737–1.371)	0.972		
UBTD1	643				
Low	321	Reference		Reference	
High	322	1.634 (1.198–2.228)	0.002	1.419 (1.016–1.980)	0.040

Table 5. The univariate and multivariate analyses of PFI.

organization, endoplasmic reticulum lumen, and basement membrane. A review of the KEGG pathways showed the enrichment of the majority of the UBTD1-associated genes in the following: protein digestion and absorption, focal adhesion, and the relaxin signaling pathway (Fig. 3B). Additionally, 1123 DEGs were found between the low- and high-expression groups with 727 and 396 up- and down-regulated genes, respectively, in the high-expression subgroup (refer to Fig. 3C). Subsequently, we conducted GO and KEGG pathway analyses. A bubble map revealed the enrichment of co-expressed DEGs in the endoplasmic reticulum lumen, extracellular structure organization, collagen-containing ECM, ECM organization, external encapsulating structure organization, collagen timer for GO pathway analysis, and staphylococcus aureus infection, protein digestion and absorption, as well as coagulation and complement cascades for KEGG pathway analysis. On the contrary, the enrichment of downregulated DEGs was primarily found in protein-DNA complex, identification of the chemical signal that contributes to the olfaction, sensory perception of smell, DNA packaging complex, nucleosome for GO pathway analysis, and alcoholism, systemic lupus erythematosus and olfactory transduction for KEGG pathway analysis (Fig. 3D). Additionally, GSEA results from the KEGG database demonstrated the correlation of UBTD1 expression upregulation with the cytokine-cytokine receptor interaction, focal adhesion, ECM receptor interaction, chemokine signaling, cell adhesion molecules cams, and leukocyte transendothelial migration pathway (Fig. 3E,F). Overall, these findings point to the potential involvement of UBTD1 in the CRC malignant progression.

UBTD1 is linked to immune infiltration in CRC

Spearman correlation was conducted to determine how UBTD1 expression correlated with several distinct types of immune cells, as measured by the CIBERSORT, EPIC, and QUAN-TISEQ. Notably, CIBERSORT showed that UBTD1 expression in CRC was linked to the infiltration levels of T cell CD4+ memory resting ($r = -0.281$, $p < 0.001$), B cell plasma ($r = -0.276$, $p < 0.001$), T cell follicular helper ($r = -0.136$, $p < 0.001$), myeloid dendritic cell activated ($r = -0.132$, $p < 0.001$), macrophage M1 ($r = 0.140$, $p < 0.001$), macrophage M2 ($r = 0.184$, $p < 0.001$), neutrophil ($r = 0.240$, $p < 0.001$) and macrophage M0 ($r = 0.276$, $p < 0.001$). Additionally, EPIC demonstrated the association UBTD1 expression in CRC with uncharacterized cell ($r = -0.498$, $p < 0.001$), T cell CD8+ ($r = -0.296$, $p < 0.001$), T cell CD4+ ($r = -0.228$, $p < 0.001$), endothelial cell ($r = 0.388$, $p < 0.001$), NK cell ($r = 0.398$, $p < 0.001$) and macrophage ($r = 0.505$, $p < 0.001$). Moreover, QUANTISEQ showed that UBTD1 expression in CRC was linked to the infiltrating levels of T cell CD4+ ($r = -0.270$, $p < 0.001$), T cell regulatory ($r = 0.155$, $p < 0.001$), T cell CD8+ ($r = 0.170$, $p < 0.001$), macrophage M1 ($r = 0.113$, $p = 0.005$) and macrophage M2 ($r = 0.189$, $p < 0.001$ (Fig. 4, Table 6). The ESTIMATE algorithm was employed to obtain the immune, stromal, and ESTIMATE scores for colorectal cancer. Individuals with high UBTD expression recorded higher scores than those with low UBTD levels, demonstrating a significant positive correlation (Fig. 5A–C).

Notably, UBTD1 expression was strongly associated with macrophages, especially M2 macrophage, which is an integral part of the TME and contributes to the modulation of angiogenesis, remodeling of the ECM, the proliferation of cancerous cells, metastases, immunosuppressive function, chemoresistance, and insensitivity to

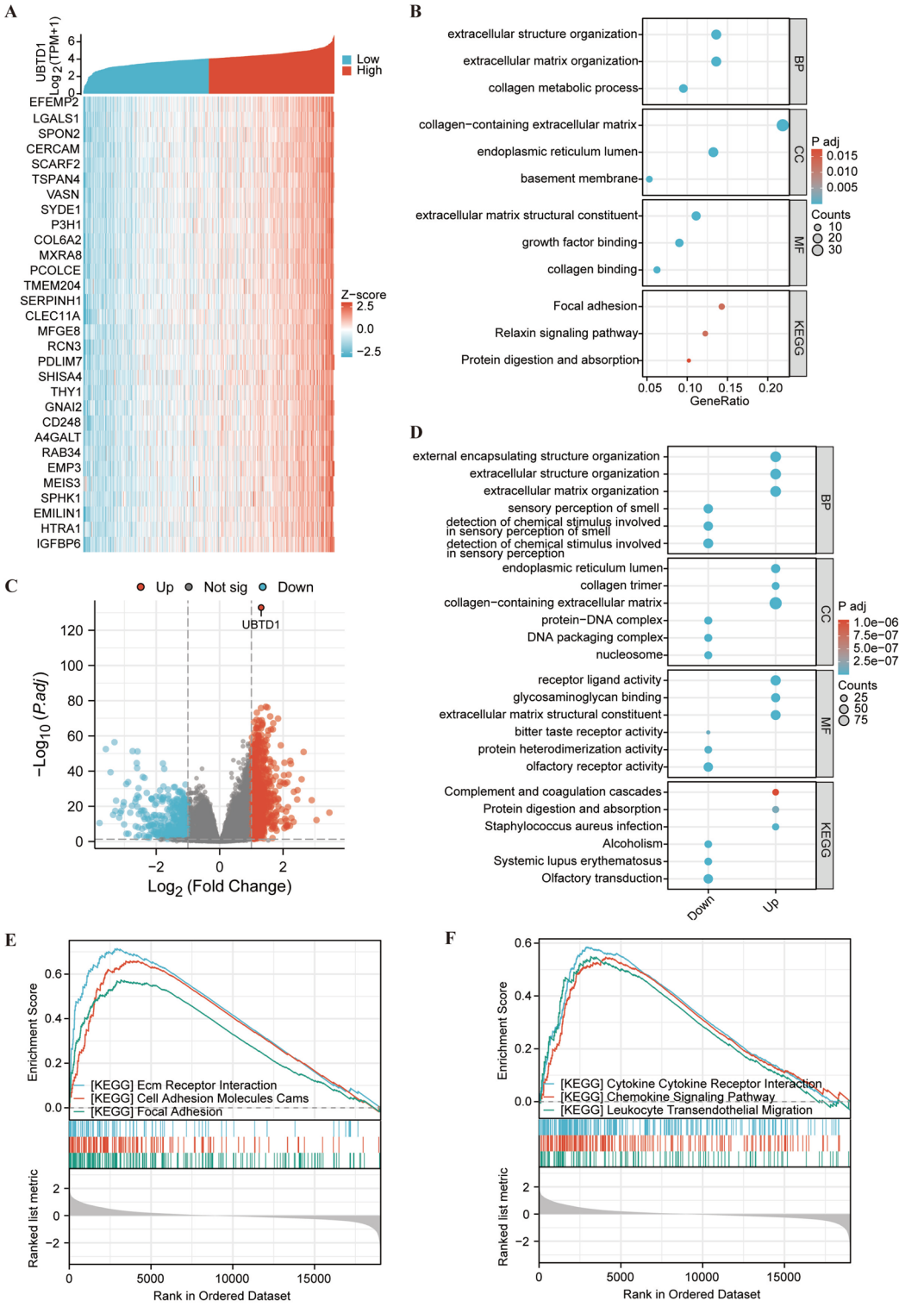

Figure 3. Functional inference of UBTD1 in CRC. (**A**) The heatmap displays the 30 top-ranked genes in CRC that have a positive correlation with UBTD1. The high and low expressions are respectively denoted by colors red and blue. (**B**) UBTD1 co-expressed gene analysis using GO and KEGG pathways. (**C**) DEGs between the low and high UBTD1 expression subgroups in CRC as shown via a volcano map. The high and low expressions are respectively denoted by colors red and blue. (D) GO and KEGG Pathway enrichment analyses for upregulated and downregulated DEGs. (**E**, **F**) GSEA enrichment plots showed correlated pathways of UBTD1.

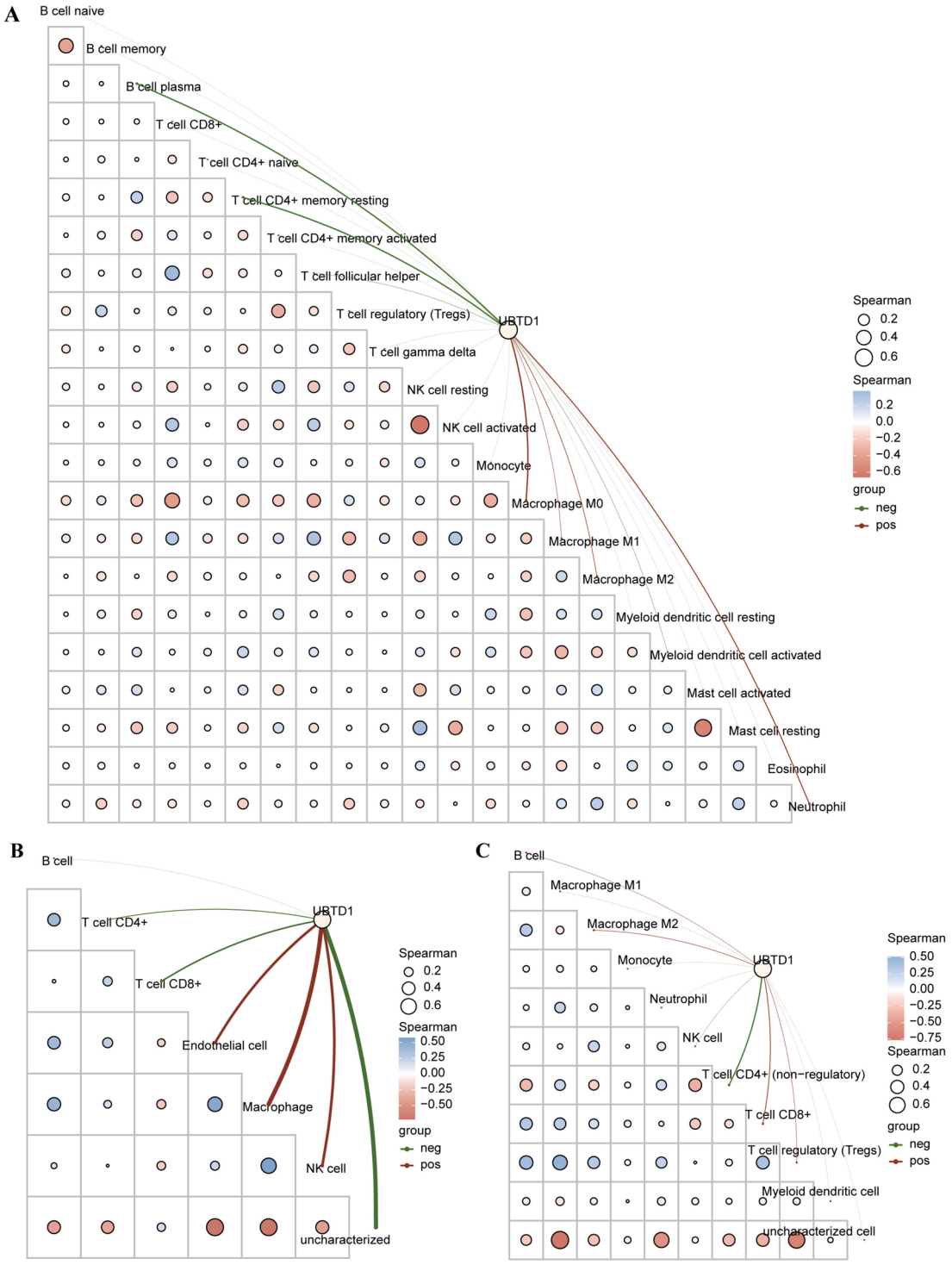

Figure 4. The association of UBTD1 expression with the levels of infiltrating immune cells and the tumor microenvironment in CRC. (**A**) The relationship between UBTD1 expression and immune cell infiltration in CRC based on CIBERSORT. (**B**) The association of UBTD1 expression with infiltrating immune cells in CRC based on QUANTISEQ. (**C**) Association of UBTD1 expression with immune cell infiltration in CRC based on EPIC.

immune checkpoint blockade treatment. The correlation of UBTD1 expression with markers associated with various subtypes of macrophages was further investigated. Our findings revealed a significantly stronger correlation between UBTD1 and M2 macrophages, as indicated by the positive associations with CD163 ($r = 0.411$, $p < 0.001$) and MRC1 ($r = 0.331$, $p < 0.001$). (Fig. 5D–F). The results of this study indicate a potential role for UBTD1 in the

Category	ID	Relevance	p value
CIBERSORT	T cell CD4+ memory resting	−0.28128	<0.001
	B cell plasma	−0.27592	<0.001
	T cell follicular helper	−0.13563	0.000709
	Myeloid dendritic cell activated	−0.13205	0.000982
	Eosinophil	−0.06588	0.101252
	T cell CD4+ memory activated	−0.06484	0.106754
	B cell naïve	−0.06451	0.108546
	T cell CD4+ naive	−0.06076	0.130708
	NK cell resting	−0.0557	0.16601
	T cell CD8+	−0.05217	0.194552
	Mast cell resting	−0.04769	0.235739
	Monocyte	−0.04615	0.251241
	Myeloid dendritic cell resting	−0.02188	0.586633
	T cell gamma delta	−0.02158	0.591668
	Mast cell activated	0.005936	0.882733
	B cell memory	0.023304	0.56248
	NK cell activated	0.034967	0.384746
	T cell regulatory (Tregs)	0.056515	0.159875
	Macrophage M1	0.139533	<0.001
	Macrophage M2	0.183907	<0.001
	Neutrophil	0.239527	<0.001
	Macrophage M0	0.275959	<0.001
EPIC	Uncharacterized cell	−0.49793	<0.001
	T cell CD8+	−0.29625	<0.001
	T cell CD4+	−0.22822	<0.001
	B cell	0.047801	0.234635
	Endothelial cell	0.387576	<0.001
	NK cell	0.39753	<0.001
	Macrophage	0.504696	<0.001
QUANTISEQ	T cell CD4+ (non-regulatory)	−0.27006	<0.001
	NK cell	−0.05679	0.157847
	Uncharacterized cell	−0.05304	0.187156
	Neutrophil	−0.03879	0.334955
	Monocyte	−0.01143	0.776299
	B cell	0.02793	0.487573
	Myeloid dendritic cell	0.063791	0.112562
	Macrophage M1	0.112592	0.005004
	T cell regulatory (Tregs)	0.154957	<0.001
	T cell CD+	0.170115	<0.001
	Macrophage M2	0.189415	<0.001

Table 6. Correlation of UBTD1 expression with immune infiltration in CRC.

transition from M1 to M2 polarization in colorectal cancer (CRC). Additionally, we compared the expression of UBTD1 with that of other genes implicated in immune regulation. Our findings demonstrate that UBTD1 expression is significantly linked to most targets within the immunological microenvironment (see Fig. 5G). The data presented in Fig. 5H demonstrates a strong correlation between transforming growth factor-beta 1 (TGFB1) and UBTD1. Additionally, analysis of Kaplan–Meier curves in Fig. 5I indicates that colorectal cancer (CRC) patients with elevated UBTD1 expression exhibit a shorter overall survival (OS) time. This observation suggests a potential mechanism by which increased UBTD1 levels may contribute to a poor prognosis in CRC. Furthermore, these findings suggest a role for UBTD1 in modulating immune infiltration in CRC.

Discussion

CRC is a complex and diverse disease, marked by alterations in cytokines that drive the disruption of various signaling pathways, ultimately contributing to the initiation, advancement, and aggressiveness of tumors. Comprehensive comprehension of the diverse developmental pathways of CRC is imperative for the detection and management of the disease, and for modifying its clinical progression[6]. The subsequent phase involves identifying a new biological marker associated with immune infiltrates and a new molecular pathway that may underpin

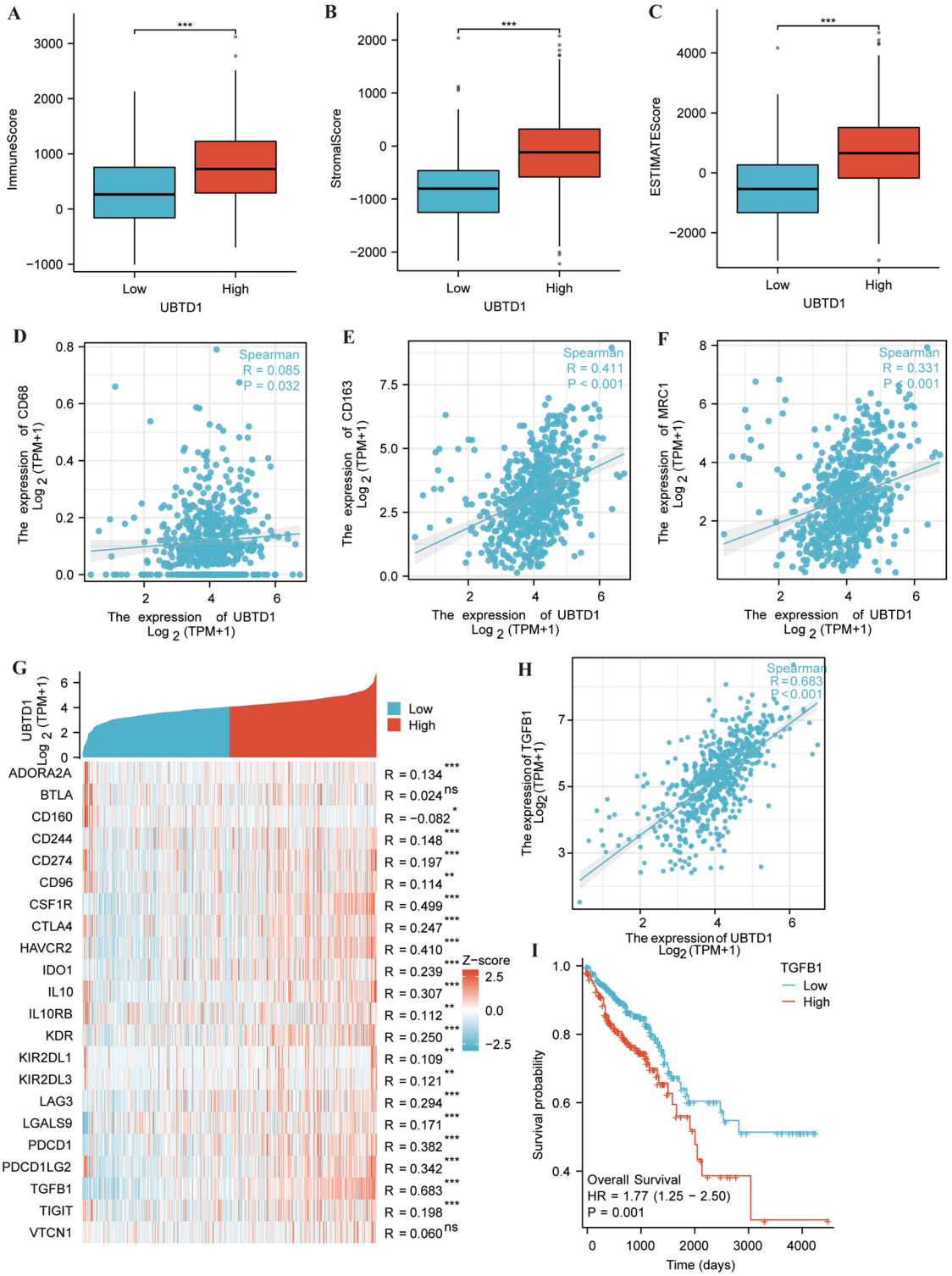

Figure 5. The correlation between UBTD1 and immune factors in CRC. (**A**–**C**) The ESTIMATE algorithm was applied to determine the association of UBTD1 expression with the ESTIMATE, stromal, and immune scores. (**D**–**F**) Expression of UBTD1 and M2 macrophage markers in CRC (**G**) Heatmap illustrating the correlations between immunoinhibitory genes and UBTD1 in CRC. (**H**) AFAP1L1 and TGFB1 expression correlation in CRC. (**I**) KM curves depicting the variation in TGFB1 expressions as a predictor of OS in CRC cases. (ns denotes no significance, *p < 0.05, **p < 0.01, ***p < 0.001).

the efficacy of immunotherapy. As mentioned in the previous part of the article, the previously research reports highlight the importance of UBTD1 in malignancies and offer potential insights into its precise function and molecular mechanisms. Nevertheless, there is a scarcity of research reports focusing on UBTD1's role in CRC. Moreover, while previous studies have predominantly suggested that UBTD1 may act as a regulator of aging by boosting p53 activity through a positive feedback loop and could potentially serve as a tumor suppressor[11], our research results deviate from the traditional understanding, thus introducing an intriguing facet to the exploration of UBTD1 in cancer.

Initially, the elevated expression of UBTD1 in CRC was validated through analysis of both database information and clinical specimens, and the comparison of differences between high and low expression samples indicates the association with various clinical and pathological features. Subsequently, an investigation into the influence of UBTD1 expression on CRC progression revealed a significant impact on OS, DSS, and PFI. Additionally, our study identified associations between UBTD1 expression and multiple immune marker genes and immune cell populations. Prior research has underscored the critical function of the immune milieu in cancer pathogenesis, with the intricate tumor microenvironment (TME) playing a pivotal function in facilitating tumor proliferation and dissemination[18]. Our research demonstrates a significant association between UBTD1 expression and macrophages. Macrophages, integral components of the mononuclear phagocytic system, are pivotal in modulating innate immunity, tissue inflammation, and homeostasis. These cells can differentiate into two different phenotypes, M1 (proinflammatory) and M2 (anti-inflammatory), with M1 phenotype bolstering the immune response against tumors and M2 macrophages fostering tumor progression through the facilitation of angiogenesis and immunosuppression[19]. Our study indicates that UBTD1 exhibits a stronger correlation with M2 macrophages in comparison with M1 macrophages, highlighting the promising value of UBTD1 in the promotion of colorectal cancer through the induction of M2 macrophages. In addition to examining the relationship between UBTD1 and DEGs, we applied GO and KEGG pathway analyses to validate UBTD1's potential role in CRC malignant progression. Based on our experimental results, GO analysis of the genes associated with UBTD1 in the top 50 indicated their involvement in extracellular matrix and structure organization, collagen metabolic processes, growth factor and collagen binding, with a predominant distribution in collagen-containing extracellular matrix, endoplasmic reticulum lumen, and basement membrane. Reviewing KEGG pathways revealed enrichment of UBTD1-associated genes in pathways such as protein digestion and absorption, focal adhesion, and the relaxin signaling pathway. Similar results were observed in the GO and KEGG analyses of the highly expressed subgroup. Some pathways, such as coagulation and complement cascades[20], protein digestion and absorption, and focal adhesion[21], have been previously shown to be related to the occurrence and development of CRC in research studies. Moreover, we investigated the mechanistic bases of UBTD1 in regulating the immune microenvironment by assessing its interactions with immune stimulation genes, immune suppression genes, and other relevant factors. Particularly noteworthy was the significant correlation observed between UBTD1 and the immune suppression gene TGFB1, which encodes the TGF-β protein known to play a pivotal role in the TGF-β pathway implicated in various malignancies[22]. Previous research[23] has demonstrated that TGFB1 contributes to the development and progression of CRC, and its upregulation has been linked to the suppression of the body's antitumor natural defense, thereby promoting tumor formation.

Our article preliminarily confirms the relationship between UBTD1 and CRC. We investigated the expression and prognostic relationship of UBTD1 in CRC using tissue samples and public database sequencing data. Furthermore, we explored the mechanism through bioinformatics methods. However, further experimental evidence is needed to fully elucidate the role of UBTD1 in CRC. This includes utilizing loss-of-function or gain-of-function models in CRC cell lines to demonstrate that UBTD1 promotes CRC malignancy, such as proliferation, migration, invasion, sphere formation, etc. Additional fundamental and clinical studies are imperative to clarify the biological value of UBTD1 and its significance in the initiation and advancement of CRC.

Conclusions

Our study findings suggest that UBTD1 exhibits elevated expression levels in CRC tissues and correlates with both advanced disease stage and unfavorable prognosis in CRC patients. Consequently, UBTD1 holds promise as a potentially valuable prognostic indicator for individuals with CRC. Further investigations, encompassing both basic research and clinical studies, are needed to comprehensively ascertain the biological significance of UBTD1 in CRC, thereby offering novel insights for the diagnosis and management of this malignancy in the future.

Data availability

All data are available in a public, open-access repository. The datasets used and/or analyzed during the current study are available in the Gene Expression Omnibus (GEO, https://www.ncbi.nlm.nih.gov/geo/) and The Cancer Genome Atlas (TCGA) network (https://cancergenome.nih.gov/).

Received: 27 March 2024; Accepted: 26 July 2024
Published online: 02 August 2024

References

1. Sung, H. *et al.* Global Cancer Statistics 2020: GLOBOCAN estimates of incidence and mortality worldwide for 36 cancers in 185 countries. *CA Cancer J. Clin.* **71**(3), 209–249 (2021).
2. Siegel, R. L., Giaquinto, A. N. & Jemal, A. Cancer statistics, 2024. *CA Cancer J. Clin.* **74**(1), 12–49 (2024).
3. Ranasinghe, R., Mathai, M. & Zulli, A. A synopsis of modern—day colorectal cancer: Where we stand. *Biochim. Biophys. Acta* **1877**(2), 188699 (2022).
4. Murphy, C. C. & Zaki, T. A. Changing epidemiology of colorectal cancer—birth cohort effects and emerging risk factors. *Nat. Rev. Gastroenterol. Hepatol.* **21**(1), 25–34 (2024).

5. Cappell, M. S., Tobi, M. & Yang, Y. X. Colonoscopy screening and colorectal cancer incidence and mortality. *N. Engl. J. Med.* **388**(4), 378 (2023).
6. Ciardiello, F. *et al.* Clinical management of metastatic colorectal cancer in the era of precision medicine. *CA Cancer J. Clin.* **72**(4), 372–401 (2022).
7. Sepulveda, A. R. *et al.* Molecular biomarkers for the evaluation of colorectal cancer: Guideline from the American Society for Clinical Pathology, College of American Pathologists, Association for Molecular Pathology, and the American Society of Clinical Oncology. *J. Clin. Oncol. Off. J. Am. Soc. Clin. Oncol.* **35**(13), 1453–1486 (2017).
8. Dagar, G., Kumar, R., Yadav, K. K., Singh, M. & Pandita, T. K. Ubiquitination and deubiquitination: Implications on cancer therapy. *Biochim. Biophys. Acta* **1866**(4), 194979 (2023).
9. Uhler, J. P. *et al.* The UbL protein UBTD1 stably interacts with the UBE2D family of E2 ubiquitin conjugating enzymes. *Biochem. Biophys. Res. Commun.* **443**(1), 7–12 (2014).
10. Yang, N. *et al.* CXCR4 mediates matrix stiffness-induced downregulation of UBTD1 driving hepatocellular carcinoma progression via YAP signaling pathway. *Theranostics.* **10**(13), 5790–5801 (2020).
11. Zhang, X. W. *et al.* UBTD1 induces cellular senescence through an UBTD1-Mdm2/p53 positive feedback loop. *J. Pathol.* **235**(4), 656–667 (2015).
12. Torrino, S. *et al.* UBTD1 regulates ceramide balance and endolysosomal positioning to coordinate EGFR signaling. *eLife.* **10**, e68348 (2021).
13. Torrino, S. *et al.* UBTD1 is a mechano-regulator controlling cancer aggressiveness. *EMBO Rep.* **20**(4), e46570 (2019).
14. Yoshihara, K. *et al.* Inferring tumour purity and stromal and immune cell admixture from expression data. *Nat. Commun.* **4**, 2612 (2013).
15. Newman, A. M. *et al.* Robust enumeration of cell subsets from tissue expression profiles. *Nat. Methods* **12**(5), 453–457 (2015).
16. Racle, J. & Gfeller, D. EPIC: A tool to estimate the proportions of different cell types from bulk gene expression data. *Methods Mol. Biol. (Clifton, NJ).* **2120**, 233–248 (2020).
17. Finotello, F. *et al.* Molecular and pharmacological modulators of the tumor immune contexture revealed by deconvolution of RNA-seq data. *Genome Med.* **11**(1), 34 (2019).
18. de Visser, K. E. & Joyce, J. A. The evolving tumor microenvironment: From cancer initiation to metastatic outgrowth. *Cancer Cell* **41**(3), 374–403 (2023).
19. Pan, Y., Yu, Y., Wang, X. & Zhang, T. Tumor-associated macrophages in tumor immunity. *Front. Immunol.* **11**, 583084 (2020).
20. Zheng, Z. *et al.* Correlation analysis between trace elements and colorectal cancer metabolism by integrated serum proteome and metabolome. *Front. Immunol.* **13**, 921317 (2022).
21. Zhu, J. *et al.* RPL21 interacts with LAMP3 to promote colorectal cancer invasion and metastasis by regulating focal adhesion formation. *Cell. Mol. Biol. Lett.* **28**(1), 31 (2023).
22. Creaney, J. *et al.* Comprehensive genomic and tumour immune profiling reveals potential therapeutic targets in malignant pleural mesothelioma. *Genome Med.* **14**(1), 58 (2022).
23. Shang, A. *et al.* Exosomal circPACRGL promotes progression of colorectal cancer via the miR-142-3p/miR-506-3p-TGF-β1 axis. *Mol. Cancer.* **19**(1), 117 (2020).

Author contributions

Zihan Zhao-Conceptualization, data curation, writing (original draft) Changjiang Yang- Conceptualization,investigation, software. visualization. Xuhua Geng- Formal analysis, methodology, validation. Congrui Yuan- Formal analysis, methodology, validation. Ruoshen Yang-software. visualization. Guibin Yang- Conceptualization, methodology, writing (review & editing).

Competing interests

The authors declare no competing interests.

Additional information

Correspondence and requests for materials should be addressed to G.Y.

Reprints and permissions information is available at www.nature.com/reprints.

Publisher's note Springer Nature remains neutral with regard to jurisdictional claims in published maps and institutional affiliations.